Creep Behavior of Fiber Reinforced Mortars and Its Effect to Reduce the Differential Shrinkage Stress

Senot Sangadji [1], Endah Safitri [1], Muhammad Z. Arifin [1], Stefanus A. Kristiawan [1*]

[1] SMARTCrete Research Group, Civil Engineering Department, Sebelas Maret University, Indonesia.

Abstract

This research aims to develop durable repair materials that can resist shrinkage cracking by exploring the role of creep in reducing shrinkage stress. In this regard, the creep effect can only be quantified if an accurate creep prediction model and theoretical analysis of the shrinkage stress in the patch repair system exist. For this purpose, the research was carried out in the following sequences: first, the research investigated the short-term creep of the patch repair materials containing accelerator and micro-synthetic fibers in the 0.00–0.12% volume fraction range. This short-term creep was measured on five-cylinder specimens (having a diameter of 75 mm and a height of 275 mm). Three specimens were used to determine the deformation of the repair material under unloading conditions, while those remaining were used to determine the total deformation under loading conditions. The amount of creep deformation was determined by taking away the unloaded (shrinkage) and instantaneous (elastic) deformations from the total deformation of the loaded specimens. Secondly, a modified prediction model of ACI 209R-08 is introduced to accurately capture the rate and magnitude of the observed creep of the repair materials. Finally, a formulated theoretical analysis of shrinkage stress in the patch repair system was proposed to examine how creep potentially reduces the repair material's cracking tendency. The results show that the asymptotic value of the creep curve is attained at an earlier age and that its magnitude is greater than that of most concrete. The modified ACI 209R-08 prediction model can closely estimate the repair materials' creep behavior. The best-fit line, residual values, and coefficient of error analyses confirm the modified model's prediction accuracy. The analysis of tensile stress development in the repair layer suggests that creep can reduce stress by up to 50%. With such a reduction, the repair material is expected to be durable in resisting shrinkage and cracking tendency.

Keywords: Creep; Fiber; Prediction Model; Repair Material; Differential Shrinkage Stress.

1. Introduction

Concrete is a relatively robust and durable construction material, so it is widely used to build various civil engineering infrastructures. Nevertheless, concrete structures often experience deterioration, which can be detected by several signs of damage, such as cracks, pop-outs, scaling, spalling, delamination, etc. The deterioration may be induced by physical or chemical processes [1]. Spalling and delamination of the concrete cover are often found on aged concrete structures that have experienced corrosion of their embedded reinforcements. These types of damage can be repaired using a patching method combined with a strengthening technique. However, some researchers have noted that the patching method might fail to restore the damaged concrete due to cracks and delamination of the patch repair material [2, 3]. These failures are closely related to the difference in the extent of shrinkage between the repair layer and the substrate concrete. The minimal existing concrete shrinkage restricts the substantial repair material shrinkage, generating multiple stresses within the repair material and at the interface bond plane [4, 5].

Repairing concrete with low-shrinkage repair materials is generally preferred as they minimize the stresses resulting from the differential shrinkage. However, almost all repair materials contain high early-strength agents to expedite the hardening process, even though some studies have shown that these agents have a negative impact on shrinkage. The use of high early-strength agents can cause the shrinkage to reach up to $500\text{-}600\times10^{-6}$ within four days of drying [6, 7]. Additionally, since the coarse aggregates are absent, the ultimate shrinkage of repair materials can be as high as 1800×10^{-6} [8]. As a result, the repair materials are prone to cracking due to potentially induced high shrinkage stress. However, other factors also influence the differential shrinkage stress development, such as the elastic modulus and creep of the repair materials. It follows that the successful development of the repair materials should not solely be concerned with obtaining mixtures to attain rapid strength of repair materials but also with assessing the interaction of all properties that will affect the durability of the repair materials.

One way to improve the durability of repair materials is to add fibers. Numerous researchers have incorporated fibers into repair material mixtures to enhance their tensile and ductility properties [9–11]. Although adding fibers can lead to improved tensile characteristics and increased resistance to cracking, the actual development of shrinkage stress can still be significant. The reason is that incorporating fibers may decrease creep [12–14], while creep is recognized as beneficial in reducing shrinkage stress. However, the fibers' influence on increasing or decreasing the creep depends on the type of fibers used. A high-stiffness fiber tends to reduce creep, and vice versa. Accordingly, using fibers with a low elastic modulus, such as polypropylene fibers, will be preferable as they positively affect tensile properties, creep, and cracking resistance [7]. Therefore, the fiber types should be carefully selected to improve the whole performance of the repair material. Once it is selected, an accurate identification, quantification, and prediction of creep of the fiber-reinforced repair materials have to be established to assess the materials' effectiveness in reducing shrinkage stress development, which potentially diminishes the cracking tendencies.

To quantify the creep behavior of fiber-reinforced mortar, it is necessary first to understand the fundamentals of creep, its influencing factors, and a predictive model that can be used to estimate creep behavior. Therefore, in the following paragraphs, the origin of creep and the fundamental factors influencing the rate and magnitude of creep are presented comprehensively. This is necessary because the creep prediction model is developed by considering these factors. Thus, any changes in the rate and magnitude of creep in a concrete/mortar mixture compared to the prediction model can be identified and traced back to these factors. Furthermore, modifying a prediction model that aligns with the observed creep rates and magnitudes will have a solid ground in such cases. In the end, the accuracy of the prediction model will affect the precision of calculating the role of creep in reducing the differential shrinkage stress.

The term 'creep' refers to a material's gradual deformation when subjected to a constant load for a prolonged period. It is plausible that the observable deformations at the macrolevel stem from the viscoelastic nature of the cement paste system at the microscopic scale [15–18]. For instance, using different types of cement with varying chemical and physical properties can cause different microstructural formations of C-S-H. Similarly, adding mineral admixtures, such as fly ash, slag, silica fume, or limestone filler, can also alter the microstructure and pore system of the concrete. The water-cement ratio is another critical factor affecting creep. A higher ratio leads to higher creep due to the concrete's larger and more interconnected pores [18–20].

The use of admixtures can also influence creep. For example, adding an accelerator to a concrete mixture can result in rapid setting due to the increased hydration and heat generation within the concrete, which subsequently increases the volume of C-S-H at an early age. Since the capillary pores of the C-S-H structure are the origin of both creep and shrinkage, while the unhydrated cement and aggregates are the inert components, the shrinkage rate of concrete increases at an early age [21]. A similar effect can be expected to occur in creep. Of course, the influence depends on the specific type and dosage of accelerator used. Using a superplasticizer in the mixture to reduce the water-cement ratio will improve the microstructure of the concrete by reducing the number of capillary pores [22, 23], which can also help minimize creep [24]. Tang et al. [25] showed that the use of superabsorbent polymers tends to increase creep, but the incorporation of shrinkage-reducing admixtures gives the opposite effect.

The type, size, and amount of the aggregates used in the concrete also affect creep. Principally, the aggregate in the concrete acts to restrain the cement paste's creep: the stiffer the aggregate, the greater the restraint provided, and vice versa. Therefore, using lightweight, recycled, or other porous aggregates can increase creep [24, 26]. A higher aggregate content can also result in lower creep rates, as the greater aggregate volume restricts the paste's deformation [27].

Adding fibers to the concrete mixture affects the creep. The effect can be complex and depend on various factors, such as the type of fiber and its volume fraction. High-elastic-modulus fibers, such as steel fibers, can result in lower creep deformation compared to concrete without fibers [13]. However, adding 2% steel fibers to the ultra-high performance concrete (UHPC) mixture causes a higher creep coefficient compared to that of a 1% fiber content. The reason for this is that the 2% fiber content causes a reduction in the concrete flowability compared to the 1% fiber content (in the low W/B ratio mixture) [27]. Meanwhile, using low-elastic-modulus fibers, such as PVA fibers, tends to increase creep [14].

The creeping behavior is influenced by humidity levels. Higher humidity can significantly reduce the creep properties of C–S–H [28]. Additionally, the curing regime also impacts creep behavior. The creep coefficient is reduced when the steam curing regime is used compared to the tempered curing regime [14].

Understanding the influencing factors, as discussed in the preceding paragraphs, is essential for predicting the time-dependent behavior of creep. Several methods have been developed for predicting the creep behavior of concrete. One such procedure is outlined in ACI 209.2R-08 [29], which offers a framework for calculating and modeling shrinkage and creep in hardened concrete. This model consists of two components that govern the time-dependent development and asymptotic value of creep, respectively, and can be expressed as Equation 1:

$$\phi_{(t,t_0)} = \frac{(t-t_0)^{\psi}}{d+(t-t_0)^{\psi}} \phi_u \tag{1}$$

where $\phi_{(t,t0)}$ is the creep coefficient, ϕ_u is the ultimate creep coefficient, t is the loading duration (days), d and ψ are constants, and t_0 is the time at first loading (days). ACI 209.2R-08 recommends that $d=10$ days and $\psi=0.6$. Both the asymptotic value, i.e., ϕ_u and the time-dependent behavior (represented by the time ratio in Equation 1) take the influence of the cement type, aggregate type, aggregate/cement ratio, water/cement ratio, humidity, temperature, and age of loading into account. In the absence of such data, ϕ_u may be assumed to be 2.35 or determined by measuring short-term creep. Once the short-term creep is obtained, then the time-dependent behavior of the investigated concrete can be extrapolated. In this way, both the time-dependent behavior and the asymptotic value can be suggested. This approach is useful for estimating the creep behavior of concrete with non-standard materials and conditions. The approach can also lead to modifying the model to suit the particular creep behavior of the investigated concrete.

The accuracy of a creep prediction model may be assessed using a best-fit line, residual values, and a coefficient of error in a similar manner to a shrinkage prediction model [6]. To determine the most suitable best-fit line, one can perform a linear regression analysis between the laboratory creep data and the projected value. The residual values (R) method computes the discrepancy between the predicted shrinkage and the laboratory creep data. If the R-value is positive, it suggests that the projected creep surpasses the test data, while a negative R-value indicates the opposite. The coefficient of error M can be obtained by utilizing the following equation:

$$M = \frac{1}{\overline{\phi(t-t_0)}} \sum \left\{ \frac{\left(\phi(t-t_0)-\phi'(t-t_0)\right)^2}{n} \right\}^{1/2} \tag{2}$$

where $\overline{\phi(t-t_0)}$ is the average creep coefficient, n represents the number of creep data, and $\phi'(t-t_0)$ is the predicted creep value.

The previous paragraphs highlighted the risk of cracking in repair material, the cause of such a risk, and the possible reduction of the risk due to the creep effect. It also discussed the factors influencing the creep and the model for estimating the creep's development with time, as well as the method to quantify the prediction accuracy. It is also important to remember that cracking occurs when the shrinkage stress exceeds the tensile capacity of the repair material. High shrinkage stress is triggered by the significant shrinkage magnitude of the repair material, mainly due to the use of an accelerator. On the other hand, the tensile capacity of the repair material can be enhanced by adding fibers. Additionally, creep can reduce tensile stress and help mitigate the risk of cracking. However, the creep effect can only be quantified if an accurate creep prediction model and theoretical analysis of the shrinkage stress in the patch repair system exist. Current creep prediction models were derived from the database of conventional concretes, which have a different evolution of creep compared to that of repair materials owing to the mixture composition. Meanwhile, a simplified analysis that can indicate stress development in the patch repair system is required to straightway assess the repair layer's shrinkage and cracking tendency. The present study develops durable repair materials containing an accelerator and micro-synthetic fibers that can be expected to resist shrinkage cracking by exploring the role of creep in reducing shrinkage stress. For this purpose, the research first investigates the short-term creep of the patch repair materials. These admixtures' effect on the repair material's creep behavior is determined. Secondly, a creep prediction model is employed to assess the long-term creep behavior, and its accuracy in estimating the repair material's creep behavior is evaluated. A modified prediction model is introduced to capture the rate and magnitude of the observed creep of the repair materials. An accurate creep prediction will help assess creep's role in reducing the shrinkage stress in the repair layer. The study also proposes a formulated theoretical analysis to examine how creep potentially reduces the repair material's cracking tendency.

The following section describes the research method covering the materials and their mixture proportion for producing the repair materials. In addition, the preparation of the creep specimens and the testing method are explained in sufficient detail. After this, the results of the creep investigation are presented and discussed. Firstly, the discussion begins with the influence of the material composition on the creep behavior and highlights the main finding of the accelerator and micro-synthetic fibers' effect on the creep. Then, the discussion moves to the accuracy of the creep prediction model to estimate the repair material's creep behavior. In this section, a modified prediction model is suggested to suit the creep behavior of the investigated repair materials. Following this, an analysis of the effect of creep

on the tensile stress development in the repair materials is presented. Finally, the conclusions section highlights the overall findings of this study, covering the influence of material composition, the accuracy of the creep prediction model, and the effect of creep on reducing the potential cracking of repair materials.

2. Research Method

2.1. Research Workflow

This study consists of three sequential works, i.e., investigating short-term creep behavior, proposing a modified creep prediction model, and analyzing shrinkage stress development in a patch repair system. Figure 1 shows the flowchart diagram indicating the details of the workflow of this research comprehensively.
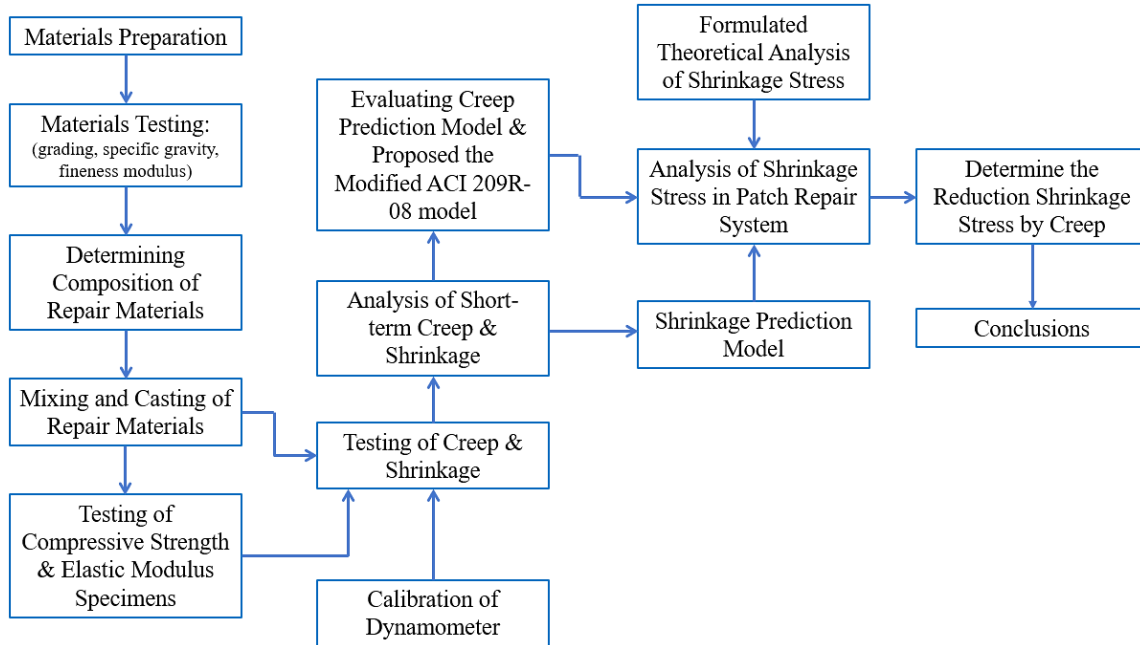
Figure 1. Research workflow

2.2. Mixtures Composition

The repair materials prepared in this research were cement-based mortars. The aggregate used was sand with a fineness modulus of 2.8, bulk specific gravity (in saturated surface dry conditions) of 2.52, and gradation within the limit of the ASTM C-33 grading curve. The sand-to-cement ratio was set at 2 through all the mixtures. The water-to-cement ratio (w/c) was 0.35, and an accelerator replaced 10% of the water to speed up the setting time and achieve high early strengths for the repair materials. The accelerator was a liquid free-chloride admixture obtained from Sika (i.e., Sika® set accelerator). The dosage used in this research was greater than the recommended dosage. The reason for this is that the repair materials were designed to have a compressive strength of 13–15 MPa after one day of age. Based on several trial mixes, the required quantity of the accelerator was found to be 10% to achieve this target strength. The researchers also utilized monofilament micro synthetic fibers to modify the repair materials' properties. The micro-fibers were added at a varying fiber volume fraction (0.0–1.2%). The properties of the micro-fibers are given in Table 1, and the mixture composition of the repair materials is summarized in Table 2.

Table 1. Properties of micro-synthetic fiber [30]

Category	Properties
Fiber class	EN 14889-2 Class 1
Raw material	100% Polyamide 6.6
Fiber type	Monofilament
Specific gravity	1.14 gr/cm^3
Length	12 mm
Filament diameter	27 mm
Tensile strength	900 MPa
Elongation at break	17.55 %
Melting point	260 ℃
Alkali resistance	Excellent
Resistance to corrosion	Excellent
Number of fibers/kg	111,000.000

Table 2. Mixtures composition

Mixture Code	Cement (kg/m^3)	Fine Aggregate (Sand) (kg/m^3)	Water (lt/m^3)	Accelerator (lt/m^3)	Micro-Synthetic Fiber (kg/m^3)
RMM 0.00%	800	1,600	200	80	0.00
RMM 0.04%	800	1,600	200	80	0.40
RMM 0.06%	800	1,600	200	80	0.60
RMM 0.08%	800	1,600	200	80	0.80
RMM 0.10%	800	1,600	200	80	1.00
RMM 0.12%	800	1,600	200	80	1.20

2.3. Specimens Preparation

Five cylindrical specimens were made for each repair material mixture. These specimens have a diameter of 75 mm and a height of 275 mm, with a height-to-diameter ratio of 3.67; this slenderness met the RILEM recommendation [31]. Three of the specimens were used to determine the deformation of the repair material under unloading conditions, while those remaining were used to determine the total deformation under loading conditions.

Once they were cast, the specimens were kept in the laboratory. On the following day, they were taken out from the molds and the still-wet surfaces of the specimens were wiped with a clean, dry cloth. Following that, four sets of DEMEC points were attached to the dry surfaces of the specimens using epoxy plastic steel adhesive. As illustrated in Figure 2, each pair of DEMEC points was positioned 200 mm apart (measured as the gauge length).
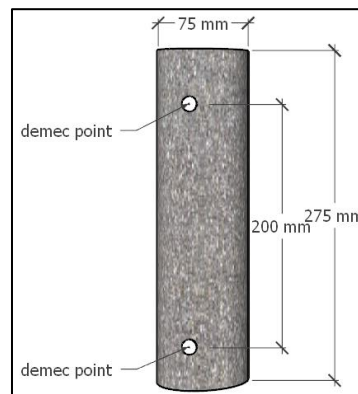

Figure 2. Creep specimen with demec points attached at a gauge length of 200 mm

In addition to the creep specimens, cube-shaped specimens were formed with dimensions of 50x50x50 mm and cylindrical specimens with dimensions of 50x100 mm. These cubes and cylindrical specimens were used to determine the repair materials' compressive strength and elastic modulus, respectively. The compressive strength value (obtained from the average of five test results) was needed to determine the applied load level (i.e., 30% of the compressive strength) on the creep specimens. Meanwhile, the elastic modulus value (obtained from the average of three test results) was used to calculate the magnitude of creep, where the amount of creep deformation was determined by taking away the unloaded (shrinkage) and the instantaneous (elastic) deformations from the total deformation of the loaded specimens.

2.4. Creep Testing

Figure 3 shows a creep loading frame where two creep specimens and a steel pipe, with an outer diameter of 275 mm, were placed in series. The ends of the specimens and the steel pipe were inserted into the circular recess of the steel plates; the recess was 275 mm in diameter and 2 mm in depth. The recess served to help position the specimens and steel pipe in line. In addition, a ball bearing connected the steel plate of the steel pipe and that of the specimen. This ball bearing helped to keep the load transfer from the steel pipe to the specimens centered.
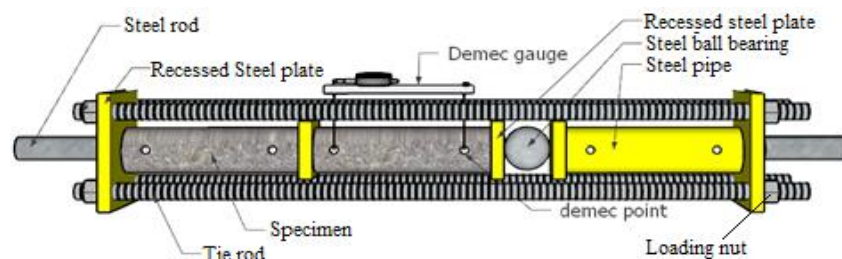

Figure 3. Arrangement of specimens in creep loading frame

The steel pipe served as a dynamometer to measure the load applied during the creep test. Four pairs of DEMEC points, with a gauge length of 200 mm, were attached to the surface of the steel pipe, similar to the creep specimens. Before being used in the creep test, the steel pipe was first calibrated by applying incremental compressive loads up to a certain magnitude. Deformation of the steel pipe was recorded at each load increment. To obtain the steel pipe's deformation, the shift in distance between the DEMEC points was gauged using a demountable mechanical strain gauge, known as the DEMEC gauge. Then, the average alteration in the length of the four pairs of DEMEC points was correlated with the load and the resulting regression equation was plotted (Figure 4). This regression equation served as a basis for determining the required load level for the creep test.
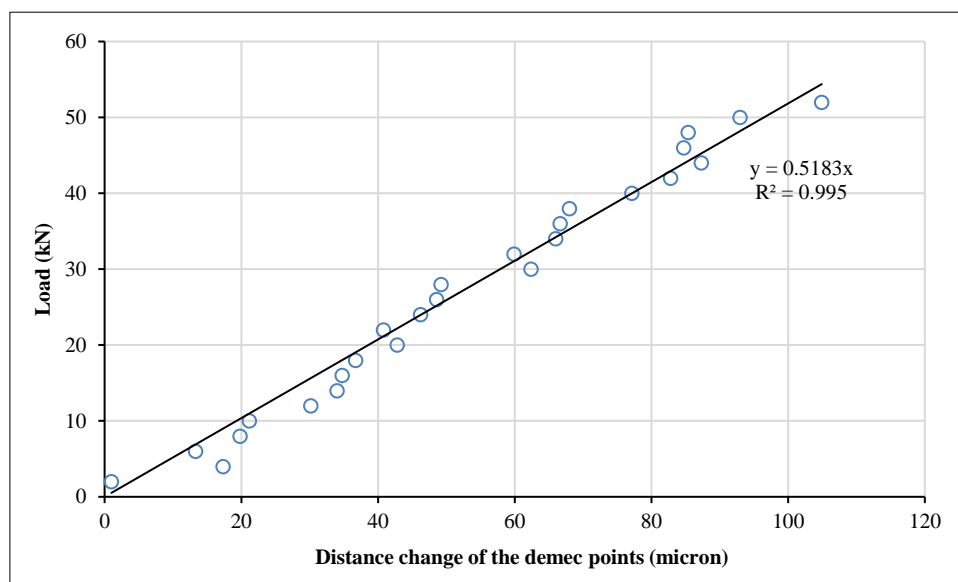

Figure 4. Relationship between distance change of DEMEC points of the steel pipe and the load

Loading for the creep test was carried out at one day of age. The loading was executed by tightening the nuts at the right end of the loading frame. Tightening these nuts caused a compressive force to be transferred from the steel plate to the steel pipe, which was then centrally transmitted to the series of specimens through the steel ball. The magnitude of the load applied was equivalent to 30% of the compressive strength of the repair material, e.g., for the RMM 0% specimen, which had a compressive strength of 13.07 MPa, the required compressive stress for the creep test was 30% x 12.75 = 3.83 MPa. If this value is converted into force (load), it will be equivalent to 3.83 MPa multiplied by the surface area of the cylindrical specimen (4,415 mm^2), which equals 16.89 kN. Based on the regression equation of Figure 4, the load corresponds to a target distance change of the DEMEC points on the steel pipe of 32.6 microns. For other mixtures, the same procedure was applied but the target sustained load was determined according to the respective compressive strength (Table 3).

Table 3. The compressive strength (1-day) of the repair materials and their respective sustained load for creep test

Mixture composition	RMM 0%	RMM 0.04%	RMM 0.06%	RMM 0.08%	RMM 0.01%	RMM 0.12%
1-day compressive strength (MPa)	12.75	14.71	14.98	14.51	14.12	13.42
Target sustained load (kN)	16.89	19.48	19.85	19.22	18.70	17.77
Target distance change (micron)	32.60	37.61	38.31	37.11	36.11	34.30

Once the load was applied, the deformation of the specimens was observed by measuring the distance change between DEMEC points attached to the surface of the specimens. This measurement was taken continuously from the day after loading, until 84 days had elapsed. Before the actual measurement, the sustained load's magnitude had to be checked. If there was a decrease in the load, the nuts needed to be re-tightened to attain the target sustained load, as before. Along with measuring the deformation of the loaded specimens, a similar measurement of the unloaded specimens was also carried out (see Figure 5). The deformation of the loaded specimens consisted of three deformations i.e., shrinkage, elastic, and creep deformation. Therefore, to separate the creep deformation from the others, the deformation of the unloaded specimen and the deformation due to the elastic properties were subtracted from the total deformation observed in the loaded specimens. The elastic deformation due to the applied sustained load can be estimated from the measured elastic modulus of the repair materials, as shown in Table 4.

Figure 5. Measurement of deformation on the unloaded (left) and loaded (right) specimen

Table 4. Elastic modulus of the repair materials

Mixture composition	RMM 0%	RMM 0.04%	RMM 0.06%	RMM 0.08%	RMM 0.01%	RMM 0.12%
1-day elastic modulus (GPa)	13.27	15.14	15.93	15.12	14.73	14.50

3. Results and Discussion

3.1. Short-Term Creep

The short-term, time-dependent deformation of the repair materials is shown in Figure 6. The total deformation represents the measured deformation on the loaded specimens due to the materials' elastic, shrinkage, and creep properties. The sudden increase in the total deformation at the start of loading indicates elastic deformation. Subsequently, the increase in total deformation with time is governed by shrinkage and creep behaviors. The shrinkage behavior of the repair materials shows a rapid increase in deformation at an early age (see Figure 6-a). After 14 days of drying, the increase is negligible as the curve approaches an asymptotic value. This behavior can be related to the materials' rapid setting and hardening processes due to using an accelerator, as noted by Sheng et al. [21]. The fast hardening process significantly reduces the drying time of the mixtures and so shortens the shrinkage needed to reach the asymptotic value. On the contrary, the creep continues to show an increase in deformation. Thus, the deformation of the repair materials at a later age (i.e., after 14 days) is dominated by creep behavior. This implies that shrinkage stress development tends to diminish after 14 days of drying, so the critical time to assess the shrinkage cracking tendency is within these 14 days.
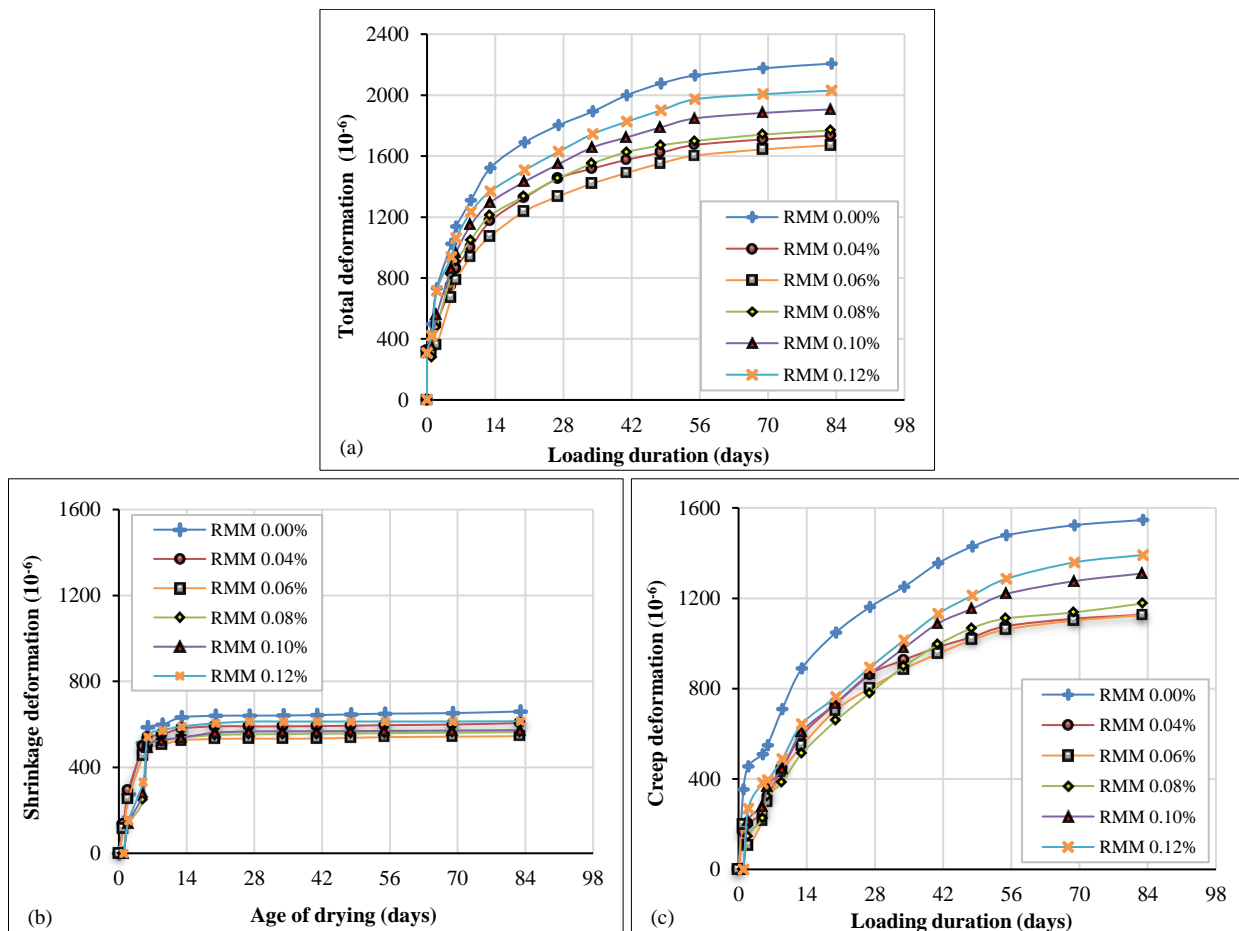

Figure 6. Short-term time-dependent deformations of the repair materials. (a) Total deformation; (b) Shrinkage; (c) Creep

The general creep behavior of the repair materials suggests that creep increases with time but at a diminishing rate. This behavior is similar to that observed by others [14]. After 56 days of loading, the creep rate slows down and the curves approach an asymptotic value. The time taken to reach this asymptotic value is longer than that of shrinkage. It seems that the compression stress applied to the repair material is still capable of forcing the moisture in the capillary pores out, causing further deformation, which cannot be achieved by insignificant drying at a later time.

The reduction of creep rate over time can be related to the aging process, which refers to the change in viscoelastic properties over time, leading to a decrease in creep in the later stages. According to the solidification theory [32], the phenomenon of creep aging is linked to the formation of fresh hydration products that exhibit non-aging creep characteristics. With the growth in the amount of hydrates, the load distribution changes, resulting in reduced creep. Bažant et al. [33] later suggested that long-term aging (microprestress-solidification theory) could be ascribed to the relaxation of microprestresses present at shear sites within nanopores. The use of an accelerator will speed up the aging process at an earlier age. Hence, the asymptotic creep behavior is attained just after 56 days. This value is considered shorter than the general creep behavior of concrete without an accelerator [24, 26, 34].

The influence of micro-fibers is to reduce the magnitude of creep. Figure 5 (c) shows that the repair materials without the inclusion of fibers exhibit greater creep than those with micro-fibers. The micro-fibers work by forming a network within the mortar, which reinforces the material and helps to distribute stress more uniformly. This can reduce the localized stress concentration, where this localized stress can cause micro-cracking and affect creep in the material. Also, the micro-fibers can help absorb energy and prevent crack propagation, reducing the potential for creep and deformation. The reduction of creep depends on the fiber volume fraction, as suggested also by Vitor et al. [13]. Too much fiber content affects compaction, increasing pores and subsequently impacting creep. Figure 7 shows the fibers' effect on creep at 84 days of loading. The figure suggests an optimum fiber volume fraction of 0.04–0.06%, resulting in the minimum creep of the repair material.
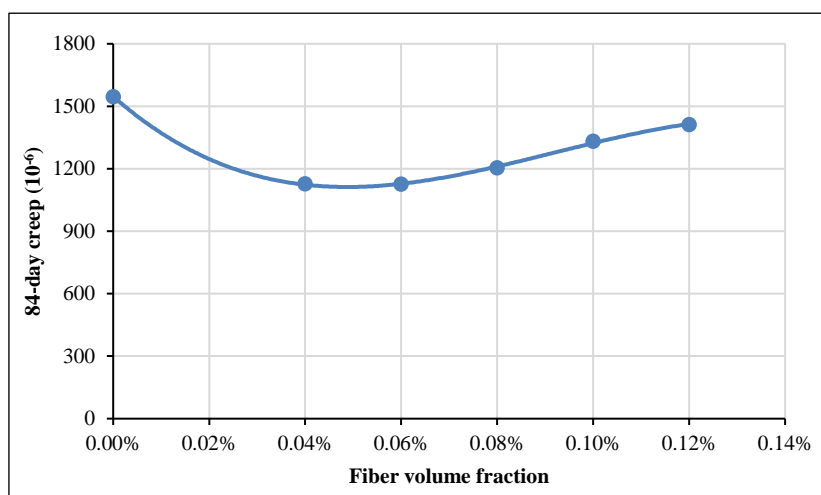

Figure 7. Effect of fiber volume fraction on 84-day creep

3.2. Prediction of Creep

Creep behavior is characterized by an increase in deformation over time, at a decreasing rate. This behavior can be formulated in a mathematical model that traces time-dependent development until the ultimate value is reached. The ACI 209R-08 model (Equation 1) expresses the development of creep over time as a time ratio, multiplied by a value representing ultimate creep. It should be noted that the model predicts creep as being expressed as a creep coefficient. The creep coefficient is a ratio between creep and elastic strain.

In this section, the ACI 209R-08 model is used to estimate the creep behavior of repair materials using short-term creep data. Figure 8 shows an example of the comparison between the predicted creep coefficient and the observed short-term creep coefficient of RMM 0.00% specimen from the laboratory investigation. The ACI 209R-08 model cannot accurately predict the creep behavior of repair materials. The inaccuracy of ACI 209R-08 in predicting the creep behavior of the repair material can be expected due to the differences in the mixture between the repair material and conventional concrete, which result in changes in the creep rate. Factors such as a higher fraction of cement paste and lower aggregate content in the repair material contribute to these differences, along with using accelerators and fibers. Delsaute et al. [19] also suggested an adapted version of prediction model (MC2010 model) to estimate the changes in the evolution of creep due to the high substitution rate of cement by limestone filler and/or slag. The mismatch between predicted and observed values is shown by an increasing deviation between the two values over time. Therefore, the time ratio and the asymptotic value of the model should be adjusted to capture the observed creep rate and its asymptotic value. The asymptotic value can be estimated more easily by extrapolating the short-term creep measurement curve. This extrapolation will provide an indication of the ultimate creep coefficient (ϕ_u) from Equation 1 and the results are presented in Table 5.
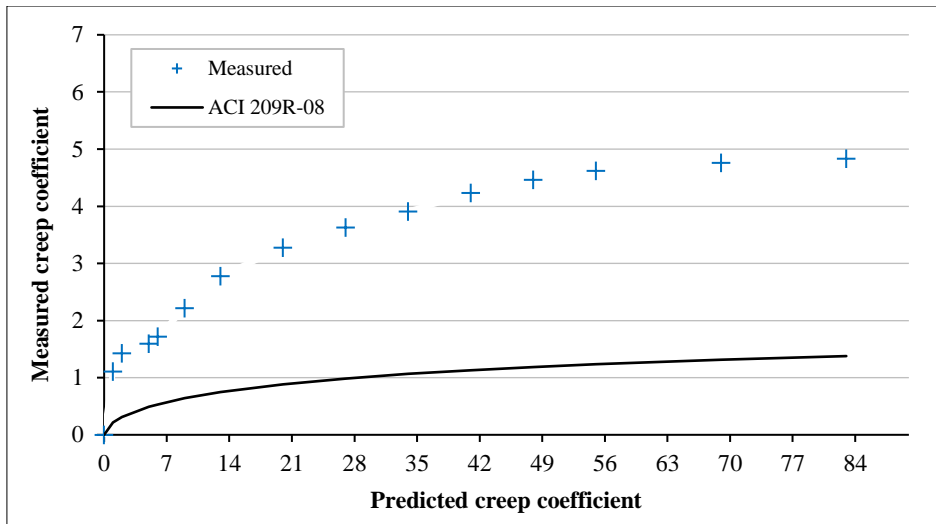
Figure 8. The predicted vs. measured creep coefficient

Table 5. Estimated the ultimate creep coefficient of the repair materials

Specimen	RMM 0.00%	RMM 0.04%	RMM 0.06%	RMM0.08%	RMM 0.10%	RMM 0.12%
ϕ_u	10.38	7.62	7.33	7.95	8.82	9.68

The ultimate creep coefficient (ϕ_u) values are much higher than those recommended by ACI 209R-08 for normal concrete, which is 2.35. The magnitude of these asymptotic values indicates that creep in repair materials is higher than that in conventional concrete. This is also consistent with the findings in Putri [35], which showed that the ultimate creep coefficient values were in the range 6-13 for various repair materials. The high values of creep coefficient in repair materials can be traced to the fact that the composition of repair materials does not contain coarse aggregates, and the aggregate/cement ratio is smaller than in concrete. Aggregates, as inert materials, play a role in resisting deformation (creep and shrinkage) originating from cement paste, and so a decrease in the number of aggregates will reduce their role in resisting deformation. Consequently, the creep coefficient values in repair materials become much higher than in normal concrete.

Referring to the asymptotic values in Table 5, the time ratio of the model can be modified by adjusting the value of d in Equation 1. After conducting several trials, the proposed constant value is $d=12$, so the following modified equation is suggested for predicting the creep behavior of the investigated repair materials:

$$\phi_{(t,t_0)} = \frac{(t-t_0)^{0.6}}{12+(t-t_0)^{0.6}} \phi_u \tag{3}$$

Figure 9 shows the prediction results using the modified ACI 209R-08 model, compared to the short-term creep coefficient measurement of the RMM 0.00% specimen. Compared to Figure 8, the prediction made using the modified model is much closer to the measured values. The accuracy of the predictions can be further evaluated by quantifying the best-fit line, residual values, and coefficient of error.
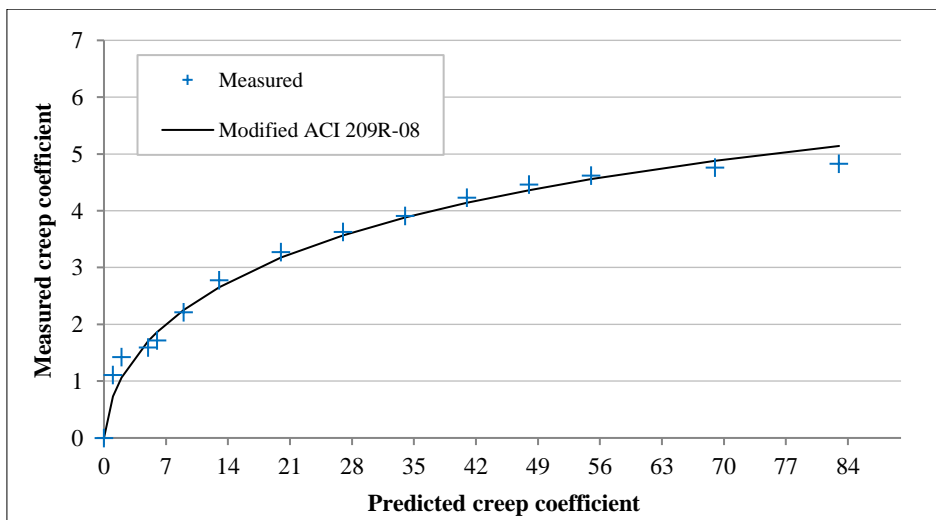

Figure 9. Creep coefficient predicted by the modified models vs. measured values

As shown in Figure 10, the best-fit line shows that ACI 209R-08 estimates the creep coefficient value at only 32% of the measured creep coefficient value (Figure 10-a). By modifying the ACI 209R-08 equation, the prediction accuracy can be improved, where the predicted value is almost the same (over 99%) as the measured creep coefficient value (Figure 10-b). The regression equation's coefficient of determination (R^2) also approaches 1, confirming a very good correlation between the predicted and measured values.

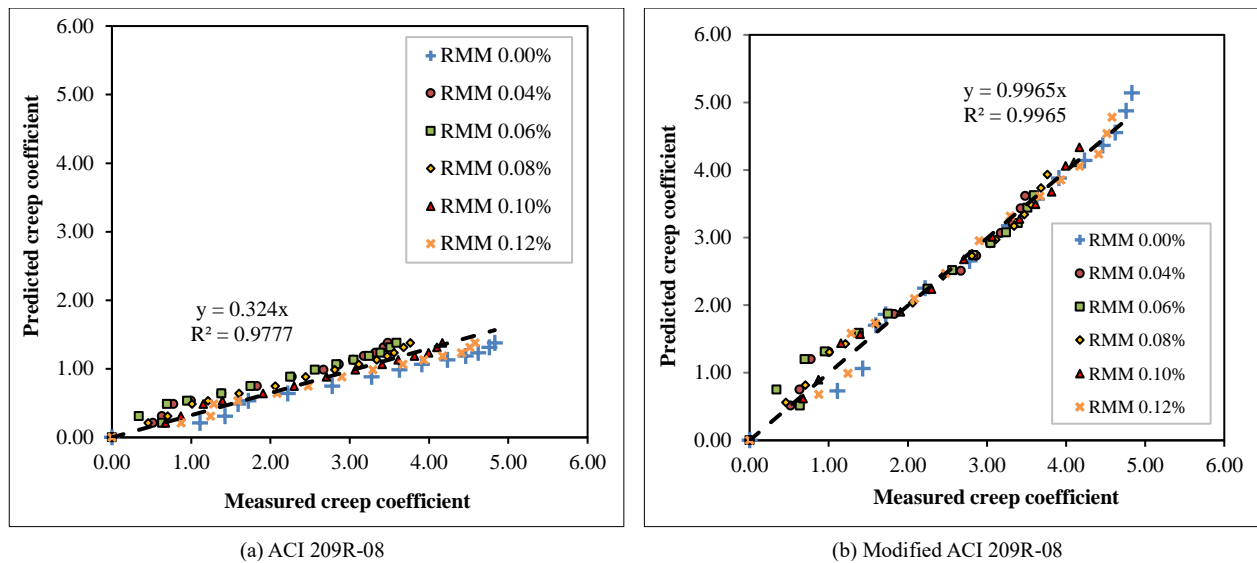(a) ACI 209R-08   (b) Modified ACI 209R-08

Figure 10. Best fit line of predicted vs. measured creep coefficient

From the analysis of residual values shown in Figure 11, the ACI 209R-08 model produces negative residual values throughout the time elapsed, indicating that the ACI model always underestimates the creep coefficient value, with the residual value reaching nearly -4. The modified ACI 209R-08 reduces the range of residual values to ±0.5. The small residual value confirms that the modified ACI 209R-08 is reasonably accurate in estimating the creep coefficient.
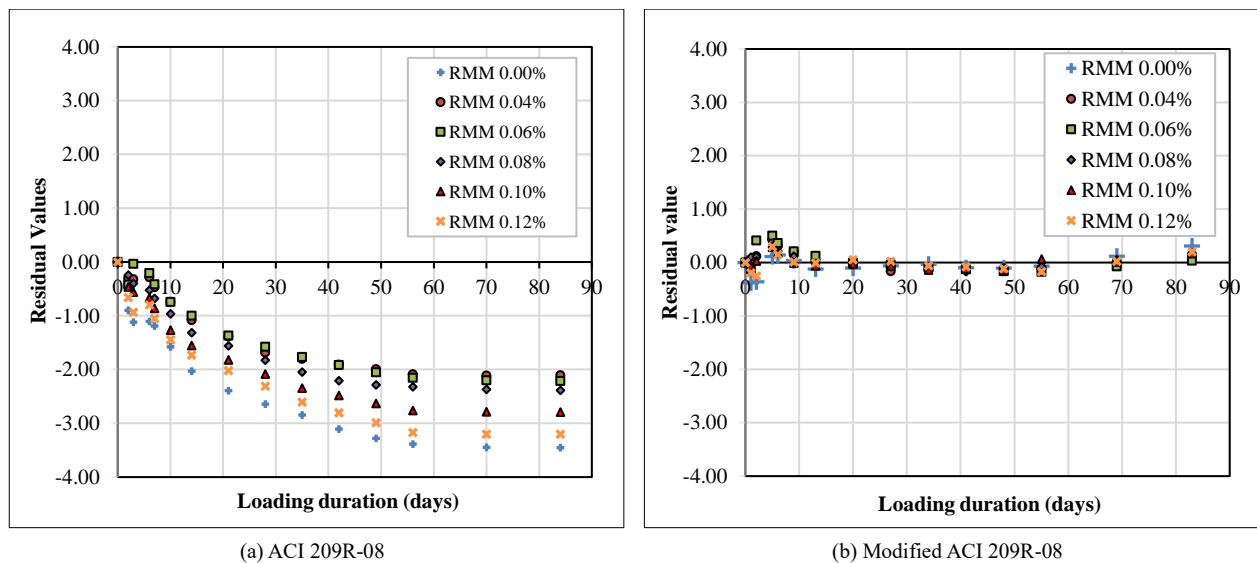

(a) ACI 209R-08   (b) Modified ACI 209R-08

Figure 11. Residual value of predicted vs. measured creep coefficient

In addition to the best-fit line and residual value analysis, the prediction accuracy is also evaluated using the coefficient of error, calculated using Equation 2. The results are presented in Table 6. A drastic decrease in the coefficient of error is obtained when the ACI 209R-08 model is modified. A coefficient of error in the range 15-31% is considered accurate

Table 6. Prediction accuracy

Method	ACI 209R-08	Modified ACI 209R-08
Best fit line	y = 0.324x	y = 0.9965x
	R^2 = 0.9777	R^2 = 0.9965
Residual value	0 to -4	-0.5 to 0.5
Coefficient of error	231%-283%	15%-31%

3.3. Creep Effect on the Reduction of Differential Shrinkage Stress

The differential shrinkage between the repair layer and the substrate concrete causes tensile stress in the repair material. This stress can cause cracking if it exceeds the tensile capacity of the repair material. Creep plays an essential role in reducing this tensile stress, so this section will analyze and discuss the effect of creep on the resistance to cracking of the repair materials. To do this, we need to examine the tensile stress in the repair layer by inspecting Figure 12.
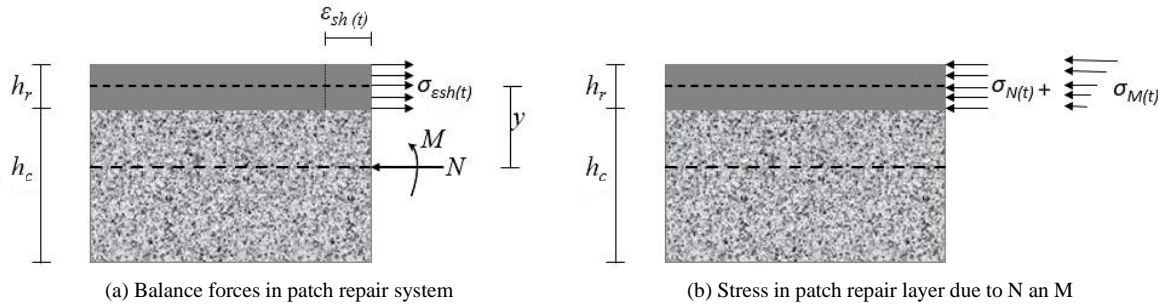

(a) Balance forces in patch repair system   (b) Stress in patch repair layer due to N an M

Figure 12. Shrinkage stress in patch repair

To simplify the analysis, it is assumed that the shrinkage of the old substrate concrete can be neglected, whereas the shrinkage of the repair material at at time t (days) is $\varepsilon_{sh(t,t0)}$. Due to a perfect interfacial bond between the repair material and substrate concrete, the substrate concrete restrains this amount of shrinkage. Consequently, a tensile stress of $\sigma_{\varepsilon sh(t)} = E_{r(t)} . \varepsilon_{sh(t)}$ is induced in the repair layer, where $E_{r(t)}$ is the elastic modulus of repair material at time t. Based on an equilibrium principle, a compressive force of $N = \sigma_{(t)} . A_r$ is required at the center of gravity (*cgc*) of the repair layer, where A_r is a cross-section of the repair material. This compressive force is equivalent to a compressive force of N at the *cgc* of the composite plus moment $M=N.y$, where y is the distance between the *cgc* of the repair layer and the composite (see Figure 12-a). Both N and M cause a compressive stress in the repair layer, $\sigma_{N(t)}$ and $\sigma_{M(t)}$ (see Figure 12-b). Hence, the total stress $\sigma_{(t)}$ at the repair layer is equal to:

$$\sigma_{(t)} = \sigma_{\varepsilon sh(t)} - \sigma_{N(t)} - \sigma_{M(t)} \tag{4}$$

Considering the elastic and creep properties of the repair material, we may adjust the first term on the right-hand side of Equation 4 and so [36]:

$$\sigma_{(t)} = \frac{E_{r(t)}}{(2+\emptyset_t)} \varepsilon_{sh(t)} - \sigma_{N(t)} - \sigma_{M(t)} \tag{5}$$

For concrete/mortar still developing with time, ageing coefficient χ is introduced in the $\frac{E_{r(t)}}{(2+\emptyset)}$ term. Hence, Equation 5 becomes:

$$\sigma_{(t)} = \frac{E_{r(t)}}{(2+\chi\emptyset_t)} \varepsilon_{sh(t)} - \sigma_{N(t)} - \sigma_{M(t)} \tag{6}$$

The range of values for χ is typically between 0.4 and 1.0, with recommended values of 0.65 to 0.80 for early-age creep and relaxation issues [37]. However, the concrete type and loading time can influence this value. For instance, the ageing coefficient of geopolymer concrete decreases from 1.0 to 0.84 when loaded on the second day after casting [38]. Equation 6 may be used at a discrete time $\Delta t_i=(t_{i+1}-t_i)$, and the total stress in the repair layer will be a cumulative of stress

$$\sigma_{(ti)} = \sum \left[\frac{E_{r(\Delta ti)}}{(2+\chi \emptyset_{\Delta ti})} \varepsilon_{sh(\Delta ti)} - \sigma_{N(\Delta ti)} - \sigma_{M(\Delta ti)} \right] \tag{7}$$

To illustrate the effect of creep on the resistance to cracking of the repair material, a simulation of stress induced by the shrinkage of repair materials was carried out. First, we took the case of a beam with a cross-section of 250 x 350 mm², where the depth ratio of the repair to the substrate layer, *hr/hc*, is 50/300. The elastic modulus of the substrate concrete, *Ec*, is 30.000 MPa, while the elastic modulus of the repair materials is given in Table 4. The shrinkage of repair materials shown in Figure 5-b was modeled as follows [6]:

$$\varepsilon_{sh(t,t_0)} = \frac{(t-t_0)}{(2+t)} \varepsilon_{shu} \tag{8}$$

where $\varepsilon_{sh(t,t_0)}$ is shrinkage at time t from the beginning of drying t_0 and ε_{shu} is the ultimate shrinkage of the repair materials. In the mean time, the creep coefficient is represented by Equation 3.

Figure 13 visualizes the difference between the two types of stress development and indicates the creep's effect in reducing stress development. Creep can reduce the tensile stresses by up to 50%, potentially delaying or dismissing the cracking in the repair materials.
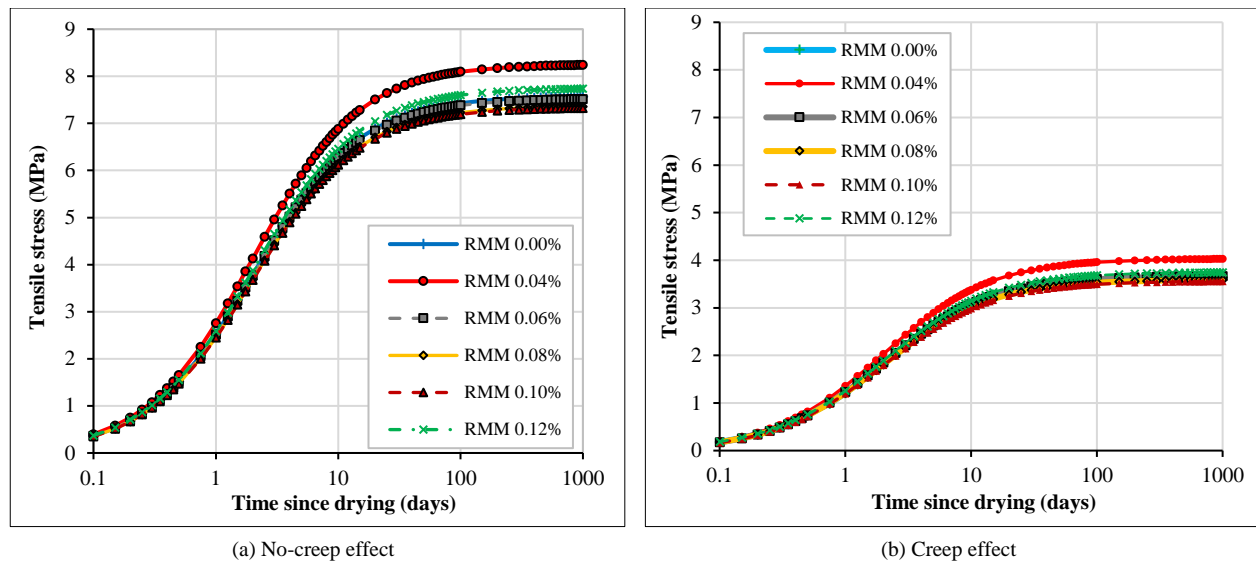
(a) No-creep effect   (b) Creep effect

Figure 13. Tensile stress development in repair materials due to differential shrinkage

4. Conclusions

The durability of repair materials containing micro-synthetic fibers and accelerators has been assessed in this study concerning their resistance against shrinkage cracking. Specifically, the study focuses on investigating the role of creep in reducing shrinkage stress in the repair layer of a patch repair system. The main conclusions that can be drawn from this research are as follows:

- The deformation of the repair materials investigated in this study indicates that it is dominated by shrinkage at an early age (14 days of drying). In contrast, at a later age, it is governed mainly by creep. This implies that shrinkage stress development tends to diminish after 14 days of drying, so the critical time to assess the shrinkage cracking tendency of the patch repair materials is within these 14 days.

- The asymptotic value of the creep curve of the repair materials is attained at an earlier age than most concrete; a rapid aging process causes this phenomenon due to the inclusion of an accelerator. Additionally, the magnitude of the creep coefficient of the repair materials is within the range of 7-11, which is higher than most concrete. This higher creep coefficient can be due to a higher volume of cement fraction and a lower aggregate content of the repair material mixture. The differences in the creep behavior of the repair materials and conventional concrete can be a good justification to propose a modified model of the ACI 209R-08 in order to accurately capture the creep rate and magnitude of the repair materials. Best-fit line, residual values, and coefficient of error analyses have confirmed the prediction accuracy of the proposed modified ACI 209R-08.

- A formulated theoretical analysis has been proposed in this research to assess the induced shrinkage stress in the repair layer. The analysis assumes a perfect bond between the repair layer and the concrete substrate; and omits the shrinkage of the concrete substrate. Although the formulated theoretical analysis has limitations due to the assumptions made, the formula can still be applied broadly for comparing the performance of various repair materials. Based on the shrinkage stress analysis of the patch repair system carried out in this study, it is indicated that creep can reduce the magnitude of the shrinkage stress development by up to 50%. With such a reduction, the repair material is expected to be durable in resisting shrinkage cracking tendency. However, it should be noted that the shrinkage and creep in this study were measured after one day of drying, so the analysis omits the earlier values, which could significantly affect the analysis results.

5. Declarations

5.1. Authors Contributions

Conceptualization: S.A.K.; methodology: S.S., E.S., and S.A.K.; investigation: M.Z.A. and E.S.; formal analysis: M.Z.A., S.S., and S.A.K.; resources: S.A.K, S.S., and E.S.; data curation: M.Z.A., S.S., and E.S.; funding acquisition: S.A.K., S.S., and E.S.; writing-original draft preparation: S.A.K. and M.Z.A.; writing-review and editing: S.S. and E.S.; visualization: M.Z.A. and S.A.K. All authors have read and agreed to the published version of manuscript.

5.2. Data Availability Statement

The data presented in this study are available on request from the corresponding author.

5.5. Conflicts of Interest

The authors declare no conflict of interest.

6. References

[1] Penttala, V. (2009). Causes and mechanisms of deterioration in reinforced concrete. Failure, Distress and Repair of Concrete Structures, 3–31, Woodhead Publishing, Sawston, United Kingdom. doi:10.1533/9781845697037.1.3.

[2] Wittmann, F. H., & Martinola, G. (2003). Durable Overlay Systems with Engineered Cementitious Composites (ECC). Restoration of Buildings and Monuments, 9(3), 235–264. doi:10.1515/rbm-2003-5760.

[3] Matthews, S. (2007). CONREPNET: Performance-based approach to the remediation of reinforced concrete structures: Achieving durable repaired concrete structures. Journal of Building Appraisal, 3(1), 6–20. doi:10.1057/palgrave.jba.2950063.

[4] Baluch, M. H., Rahman, M. K., & Al-Gadhib, A. H. (2002). Risks of Cracking and Delamination in Patch Repair. Journal of Materials in Civil Engineering, 14(4), 294–302. doi:10.1061/(asce)0899-1561(2002)14:4(294).

[5] Zhou, J., Ye, G., Schlangen, E., & van Breugel, K. (2008). Modelling of stresses and strains in bonded concrete overlays subjected to differential volume changes. Theoretical and Applied Fracture Mechanics, 49(2), 199–205. doi:10.1016/j.tafmec.2007.11.006.

[6] Safitri, E., Kusworo, R. A., & Kristiawan, S. A. (2023). Shrinkage of Micro-Synthetic Fiber-Reinforced Mortar. Infrastructures, 8(1), 7. doi:10.3390/infrastructures8010007.

[7] Shen, D., Liu, C., Luo, Y., Shao, H., Zhou, X., & Bai, S. (2023). Early-age autogenous shrinkage, tensile creep, and restrained cracking behavior of ultra-high-performance concrete incorporating polypropylene fibers. Cement and Concrete Composites, 138, 104948. doi:10.1016/j.cemconcomp.2023.104948.

[8] Yücel, H. E., Dutkiewicz, M., & Yıldızhan, F. (2022). Application of ECC as a Repair/Retrofit and Pavement/Bridge Deck Material for Sustainable Structures: A Review. Materials, 15(24), 8752. doi:10.3390/ma15248752.

[9] Banthia, N., Gupta, R., & Mindess, S. (2006). Development of fiber reinforced concrete repair materials. Canadian Journal of Civil Engineering, 33(2), 126–133. doi:10.1139/l05-093.

[10] Bhutta, A., Farooq, M., & Banthia, N. (2019). Performance characteristics of micro fiber-reinforced geopolymer mortars for repair. Construction and Building Materials, 215, 605–612. doi:10.1016/j.conbuildmat.2019.04.210.

[11] Zanotti, C., Rostagno, G., & Tingley, B. (2018). Further evidence of interfacial adhesive bond strength enhancement through fiber reinforcement in repairs. Construction and Building Materials, 160, 775–785. doi:10.1016/j.conbuildmat.2017.12.140.

[12] Liu, C., Shen, D., Yang, X., Shao, H., Tang, H., & Cai, L. (2023). Early-age properties and shrinkage induced stress of ultra-high-performance concrete under variable temperature and uniaxial restrained condition. Construction and Building Materials, 384, 131382. doi:10.1016/j.conbuildmat.2023.131382.

[13] Pena, P. V. C., Ferreira, R. A. dos R., Santos, A. C. dos, & Oliveira, A. M. de. (2023). Analysis of the compressive creep strain of the concretes with steel fibers: A holistic view in micro and macro scale. Journal of Building Engineering, 71, 106436. doi:10.1016/j.jobe.2023.106436.

[14] Huang, Y., Wang, J., Wei, Q., Shang, H., & Liu, X. (2023). Creep behaviour of ultra-high-performance concrete (UHPC): A review. Journal of Building Engineering, 69, 106187. doi:10.1016/j.jobe.2023.106187.

[15] Acker, P., & Ulm, F. J. (2001). Creep and shrinkage of concrete: Physical origins and practical measurements. Nuclear Engineering and Design, 203(2–3), 143–158. doi:10.1016/S0029-5493(00)00304-6.

[16] Wyrzykowski, M., Scrivener, K., & Lura, P. (2019). Basic creep of cement paste at early age - the role of cement hydration. Cement and Concrete Research, 116, 191–201. doi:10.1016/j.cemconres.2018.11.013.

[17] Suwanmaneechot, P., Aili, A., & Maruyama, I. (2020). Creep behavior of C-S-H under different drying relative humidities: Interpretation of microindentation tests and sorption measurements by multi-scale analysis. Cement and Concrete Research, 132, 106036. doi:10.1016/j.cemconres.2020.106036.

[18] Gan, Y., Romero Rodriguez, C., Zhang, H., Schlangen, E., van Breugel, K., & Šavija, B. (2021). Modeling of microstructural effects on the creep of hardened cement paste using an experimentally informed lattice model. Computer-Aided Civil and Infrastructure Engineering, 36(5), 560–576. doi:10.1111/mice.12659.

[19] Delsaute, B., Torrenti, J. M., & Staquet, S. (2021). Prediction of the basic creep of concrete with high substitution of Portland cement by mineral additions at early age. Structural Concrete, 22(S1), E563–E580. doi:10.1002/suco.201900313.

[20] Kristiawan, S. A., & Nugroho, A. P. (2017). Creep Behaviour of Self-compacting Concrete Incorporating High Volume Fly Ash and its Effect on the Long-term Deflection of Reinforced Concrete Beam. Procedia Engineering, 171, 715–724. doi:10.1016/j.proeng.2017.01.416.

[21] Sheng, Y., Xue, B., Li, H., Qiao, Y., Chen, H., Fang, J., & Xu, A. (2017). Preparation and Performance of a New-Type Alkali-Free Liquid Accelerator for Shotcrete. Advances in Materials Science and Engineering, 2017. doi:10.1155/2017/1264590.

[22] Zhang, Y., & Kong, X. (2014). Influences of superplasticizer, polymer latexes and asphalt emulsions on the pore structure and impermeability of hardened cementitious materials. Construction and Building Materials, 53, 392–402. doi:10.1016/j.conbuildmat.2013.11.104.

[23] Huang, H., Qian, C., Zhao, F., Qu, J., Guo, J., & Danzinger, M. (2016). Improvement on microstructure of concrete by polycarboxylate superplasticizer (PCE) and its influence on durability of concrete. Construction and Building Materials, 110, 293–299. doi:10.1016/j.conbuildmat.2016.02.041.

[24] Cartuxo, F., De Brito, J., Evangelista, L., Jiménez, J. R., & Ledesma, E. F. (2015). Rheological behaviour of concrete made with fine recycled concrete aggregates - Influence of the superplasticizer. Construction and Building Materials, 89, 36–47. doi:10.1016/j.conbuildmat.2015.03.119.

[25] Tang, C., Dong, R., Tang, Z., Long, G., Zeng, X., Xie, Y., Xie, Y., Cheng, G., Ma, G., Wang, H., & Wei, Y. (2023). Effects of shrinkage reducing admixture and internal curing agent on shrinkage and creep of high performance concrete. Journal of Building Engineering, 71, 106446. doi:10.1016/j.jobe.2023.106446.

[26] Hong, S. H., Choi, J. S., Yuan, T. F., & Yoon, Y. S. (2023). A review on concrete creep characteristics and its evaluation on high-strength lightweight concrete. Journal of Materials Research and Technology, 22, 230–251. doi:10.1016/j.jmrt.2022.11.125.

[27] Xu, Y., Liu, J., Liu, J., Zhang, Q., & Zhao, H. (2019). Creep at early ages of ultrahigh-strength concrete: Experiment and modelling. Magazine of Concrete Research, 71(16), 847–859. doi:10.1680/jmacr.17.00551.

[28] Liu, Y., Li, Y., Jin, C., Li, H., & Mu, J. (2023). Research on irrecoverable creep of the hardened cement paste under different relative humidity. Journal of Building Engineering, 69(100), 106276. doi:10.1016/j.jobe.2023.106276.

[29] ACI 209.2R-08. (2008). Guide for Modeling and Calculating Shrinkage and Creep in Hardened Concrete. American Concrete Institute (ACI), Michigan, United States.

[30] Technical Data Sheet. (2023). KraTos Micro 12 mm. Kordsa, İzmit, Turkey. Available online: https://img1.wsimg.com/blobby/go/009e9e51-e2ed-4c41-b640-0c82b1d83403/downloads/KraTos Micro 12 mm Polyamide Fiber (Findotek).pdf?ver=1656229786934 (accessed on June 2023).

[31] RILEM Technical Committees 129. (2000). Part 8: Steady-state creep and creep recovery for service and accident conditions. Materials and Structures, 33(1), 6–13. doi:10.1007/bf02481690.

[32] Bažant, Z. P., & Prasannan, S. (1988). Solidification theory for aging creep. Cement and Concrete Research, 18(6), 923–932. doi:10.1016/0008-8846(88)90028-2.

[33] Bažant, Z. P., Hauggaard, A. B., Baweja, S., & Ulm, F. J. (1997). Microprestress-solidification theory for concrete creep. I: Aging and drying effects. Journal of engineering mechanics, 123(11), 1188-1194. doi:10.1061/(ASCE)0733-9399(1997)123:11(1188).

[34] Chen, Y., Liu, P., Sha, F., Yu, Z., He, S., Xu, W., & Lv, M. (2022). Effects of Type and Content of Fibers, Water-to-Cement Ratio, and Cementitious Materials on the Shrinkage and Creep of Ultra-High Performance Concrete. Polymers, 14(10), 1956. doi:10.3390/polym14101956.

[35] Putri, P. M. (2021). Study of mortar creep with additional polymer materials for concrete repair. Journal of Physics: Conference Series, 1912(1), 012061. doi:10.1088/1742-6596/1912/1/012061.

[36] Kristiawan, S. A. (2012). Evaluation of Models for Estimating Shrinkage Stress in Patch Repair System. International Journal of Concrete Structures and Materials, 6(4), 221–230. doi:10.1007/s40069-012-0023-y.

[37] Gilbert, R. I., & Ranzi, G. (2010). Time-dependent behaviour of concrete structures. CRC Press, London, United Kingdom. doi:10.1201/9781482288711.

[38] Cheng, Z. Q., Zhao, R., Yuan, Y., Li, F., Castel, A., & Xu, T. (2020). Ageing coefficient for early age tensile creep of blended slag and low calcium fly ash geopolymer concrete. Construction and Building Materials, 262, 119855. doi:10.1016/j.conbuildmat.2020.119855.